

Hydrogen storage in proton-conductive perovskite-type oxides and their application

Shaimaa Mohamed abdel-all Ibrahim^{†*}

Chemistry Department, Faculty of Science and Arts, Al Qassim University, Buraidah, Saudi Arabia
(Received 20 November 2013 • accepted 14 March 2014)

Abstract—Various mixed oxides having perovskite structure were prepared by co-precipitation and sol-gel methods. The samples were calcined at 700 °C. The produced solids were characterized using X-ray diffraction analysis (XRD), thermogravimetry (TGA), differential thermal analysis (DTA), high resolution transmission electron microscope (HRTEM), nitrogen adsorption at -196 °C and hydrogen adsorption isotherms conducted at 100 °C. The results revealed the formation of nanosized mixed solids, namely LaNiO₃, LaFeO₃, LaCoO₃, LaCu₂O₄ and LaCrO₃ compounds with crystallite size within 27-37 nm. The hysteresis loop of nitrogen adsorption isotherms of different investigated adsorbents indicate clearly the porous nature of different solids calcined at 700 °C. The most active candidate towards hydrogen uptake is LaNiO₃ prepared via sol-gel technique. Its adsorption capacity measured at 100 °C and 20 bar hydrogen pressure attained 1.7 wt%. So, LaNiO₃ prepared via sol-gel technique could be considered as very promising material for hydrogen storage.

Keywords: Perovskite, Coprecipitation, Sol-gel, Hydrogen Storage, Nano Material

INTRODUCTION

Technological advancement and growing world economies have led to major improvements in the living conditions of people in the hoped world, but oil, coal, and natural gas have caused a relatively recent and dramatic buildup of greenhouse gases in the atmosphere, most notably CO₂ [1,2]. This environmental imperative requires us to quickly come to terms with the actual costs, including environmental externalities, of all of our energy use. Only then will the economic reality of energy consumption be realized and renewable sources expand through true market forces. Fossil fuels like oil, natural gas, and coal do have a future in helping to meet this growing demand [3], but the global demand for energy and call for tougher environmental legislation have pointed to the need of developing eco-friendlier technologies that can meet the increased energy demand [4].

Hydrogen has been touted as the basis of a new and powerful energy economy not reliant on fossil fuels. The use of hydrogen as an energy carrier suitable to replace gasoline and other fossil fuels has been widely discussed as a way toward sustainable fuel. The design of hydrogen storage materials is one of the principal challenges that must be met before the development of a hydrogen economy. While hydrogen has a large specific energy, its volumetric energy density is so low as to require development of materials that can store and release it when needed. While much of the research on hydrogen storage focuses on metal hydrides, some of these materials are currently limited by slow kinetics and energy inefficiency. Catalysis is one of the critical factors in the improvement of hydrogen sorption kinetics in these metal hydride systems. For exam-

ple, the poor kinetics of MgH₂ was greatly improved by addition of different oxide catalysts that enhance hydriding properties at relatively low temperature, such as V₂O₅ [5]. However, systems based on these materials have an inherent heat problem. This problem is due to the large hydrogenation enthalpy (typically greater than 33 kJ/mol H₂) characteristic of metal hydrides reversible at around 100 °C [6]. Nano-structured materials with high surface area are actively being developed as another option [1]. Hydrogen storage in nanoporous material is a physical storage approach [4] that includes compressed or liquefied molecular hydrogen and hydrogen adsorbed in the pores of the material. Some of the most common materials considered for hydrogen storage include porous carbon [3], zeolites [4], metal-organic frameworks [7,8] and perovskite [9-12].

A wide variety of solids that include metals and intermetallics forming hydrides have been investigated for hydrogen storage [13,14]. Mandal et al. [14] showed that alkaline earth manganites, BaMnO₃/Pt reversibly adsorbs ≈1.25 mass% of hydrogen in the temperature range 190-260 °C at atmosphere pressure. Perovskite-type oxides which are reported herein as hydrogen uptake materials could be considered to be one of the valuable alternative materials. This is because perovskite oxides are cheaper, thermally stable and comparatively active [15,16].

Also, perovskite have been considered as prototype material for fundamental areas of solid state chemistry, physics and catalysis. The advantages of perovskite catalysts are as follows [17]: (i) Wide variety of composition and constituent elements keeping essentially the basic structure unchanged. (ii) Bulk structure can be characterized well. The surface can be fairly well estimated taking advantage of this well-defined bulk structure. (iii) Valency, stoichiometry and vacancy can be varied widely so enhancing their catalytic activity. (iv) Huge information on physical and solid-state chemical properties has been accumulated. (v) Increasing the thermal stability of the transition metal oxides.

The present work aimed at investigating the effect of methods

[†]To whom correspondence should be addressed.

E-mail: shiamaa_332003@yahoo.com

^{*}Permanent address: Chemistry Department, Faculty of Education, Ain Shams University, Cairo, Egypt.

Copyright by The Korean Institute of Chemical Engineers.

of preparation on physicochemical, surface properties and hydrogen uptake on different perovskite oxides. The techniques employed were XRD, DTA, TGA, nitrogen adsorption at $-196\text{ }^{\circ}\text{C}$, transmission electron microscope (TEM) and kinetics of hydrogen isotherms measured at $100\text{ }^{\circ}\text{C}$.

EXPERIMENTAL

1. Materials

The chemicals employed were of analytical grade as supplied by Aldrich and Merck companies. LaNiO_3 has been synthesized by sol-gel and co-precipitation methods:

1-1. Sol-gel Method

Lanthanum nitrate [$\text{La}(\text{NO}_3)_3 \cdot 6\text{H}_2\text{O}$], nickel nitrate [$\text{Ni}(\text{NO}_3)_2 \cdot 6\text{H}_2\text{O}$], ferric, cobalt, copper, or chromium nitrate and citric acid were mixed and stirred for 1 h. Water was evaporated from the mixed solution at $100\text{ }^{\circ}\text{C}$, until a viscous gel was obtained. The gel was kept at $110\text{ }^{\circ}\text{C}$ over-night and the resultant mass was then calcined at $700\text{ }^{\circ}\text{C}$ for 5 h in air.

1-2. Co-precipitation Method

The co-precipitation process was applied at fixed pH and definite temperature using a certain volume of lanthanum nitrate, and a certain volume of nickel, ferric, cobalt, copper, or chromium nitrate with dropwise addition of NaOH solution (1 M). The rate of dropping of mixed nitrates and sodium hydroxide solutions was controlled to keep the pH of co-precipitation medium constant at a fixed pH value. The carefully washed precipitate was dried at $110\text{ }^{\circ}\text{C}$ till constant weight, and then subjected to heating at $700\text{ }^{\circ}\text{C}$ for 5 h in air.

2. Techniques

X-ray powder diffractograms of investigated samples calcined at $700\text{ }^{\circ}\text{C}$ were determined using a Bruker diffractometer (Bruker D_8 advance target) the scan rate was fixed at 8° in $2\theta\text{ min}^{-1}$ for phase identification and 0.8° in $2\theta\text{ min}^{-1}$ for line broadening profile analysis, respectively.

The patterns were run with Cu $K\alpha 1$ with second monochromator ($\lambda=0.1545\text{ nm}$) at 40 kV and 40 mA. The crystallite size of crystalline phases present in different solids investigated was calculated from the line broadening of the main diffraction lines of these phases using the Scherrer equation [18]:

$$d = \frac{k\lambda}{\beta_{1/2} \cos \theta}$$

where “d” is the mean crystallite diameter in \AA , “ λ ” the X-ray wavelength, “k” the Scherrer constant (0.89), “ $\beta_{1/2}$ ” the full-width at half-maximum (FWHM), of the main diffraction peak expressed in radian of crystalline phases and “ θ ” is the diffraction angle.

Differential thermal analysis (DTA) of the different un-calcined samples was carried out using Perkin-Elmer DTA thermal analyzer. An 8 mg solid specimen was taken in each experiment. The rate of heating was kept at $10\text{ }^{\circ}\text{C min}^{-1}$. Thermogravimetry (TGA) involved a Perkin-Elmer (TGA7) thermogravimetric analyzer, with the rate of heating kept at $10\text{ }^{\circ}\text{C/min}$.

The microstructure of the samples was examined for very dilute suspensions in water using JEOL JEM-1230 transmission electron microscope (TEM) with acceleration voltage of 80 kV. The microscopy probes of the sample were prepared by adding a small drop

of the water dispersions onto a Lacey carbon film-coated copper grid and allowed to dry initially in air, then by applying high vacuum.

The different surface characteristics, namely specific surface area (S_{BET}) and total pore volume (V_p) and mean pore radius (r) of the various adsorbents, were determined from analysis of nitrogen adsorption-desorption isotherms measured at $196\text{ }^{\circ}\text{C}$ using Quantachrome NOVA automated gas sorbometer. The values of V_p were computed from the relation:

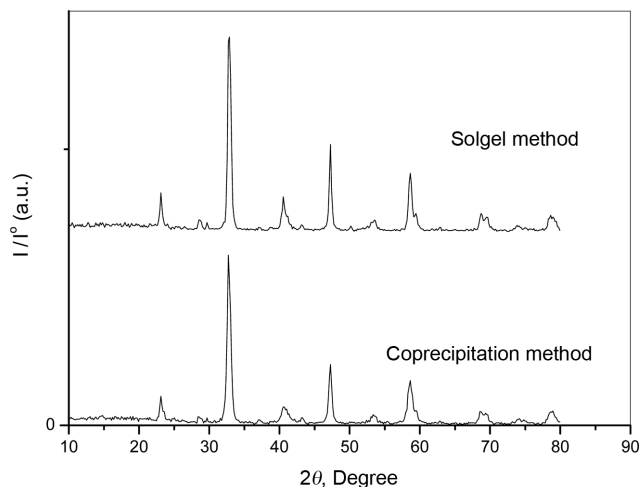


Fig. 1. X-ray diffractograms of LaNiO_3 solids prepared by coprecipitation and sol gel being calcined at $700\text{ }^{\circ}\text{C}$.

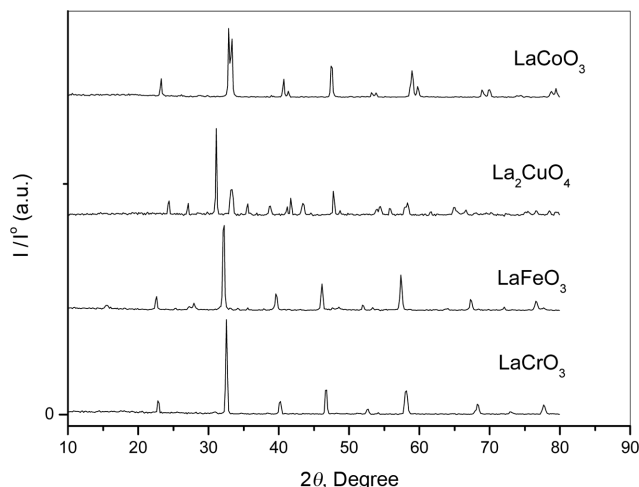


Fig. 2. X-ray diffractograms of LaCrO_3 , LaFeO_3 , LaCu_2O_4 and LaCoO_3 solids prepared by coprecipitation and being calcined at $700\text{ }^{\circ}\text{C}$.

Table 1. Crystallite size of different oxides being calcined at $700\text{ }^{\circ}\text{C}$

Solids	Crystallite size (nm)
LaNiO_3 (coprecipitation)	32
LaNiO_3 (sol-gel)	29
LaFeO_3	33
LaCoO_3	27
LaCrO_3	37
LaCu_2O_4	34

$$V_p = 15.45 \times 10^{-4} \times V_{st} \text{ cm}^3/\text{g}$$

where V_{st} is the volume of nitrogen adsorbed at P/P^0 tends to unity. The values of r^- were determined from Eq.

$$r^- = 2V_p/S_{BET} \times 10^4 \text{ \AA}$$

The hydrogen adsorption capacity of different solids was determined by the measurement of pressure-composition isotherms (PCI) by volumetric method using AMC PCI-HP 1200 equipment. Temperature was controlled with a precision of ± 0.1 °C. The accuracy of hydrogen content measurements was ± 0.04 wt%. To minimize contamination from air the material under investigation was degassed

at 200 °C for 1 h under dynamic vacuum before test. Pressure-composition isothermal (PCI) plots were traced under the above-mentioned conditions.

RESULTS AND DISCUSSION

1. XRD and TEM Measurements

The XRD patterns of the prepared solids calcined at 700 °C are depicted in Figs. 1 and 2. However, the crystallite size of different solids was determined from Scherrer's equation [18] and given in Table 1. Examination of Figs. 1 and 2 and Table 1 reveals (i) The presence of rather well crystallized rhombohedral perovskite phase;

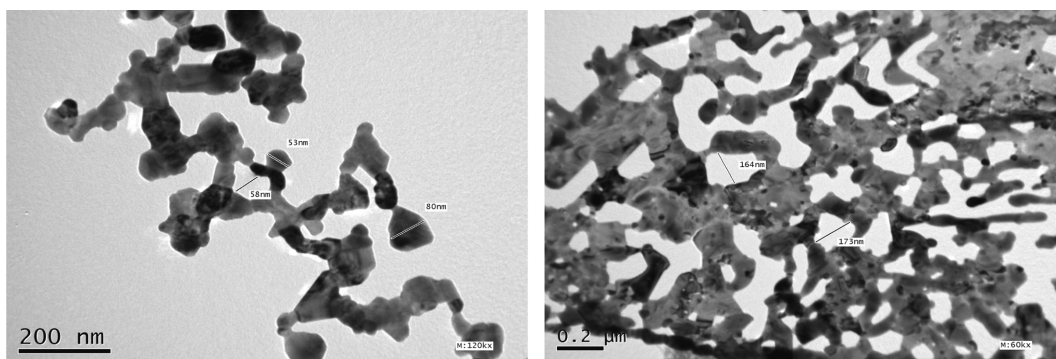


Fig. 3. TEM micrograph of LaNiO_3 and LaCu_2O_4 solids prepared by coprecipitation and being calcined at 700 °C.

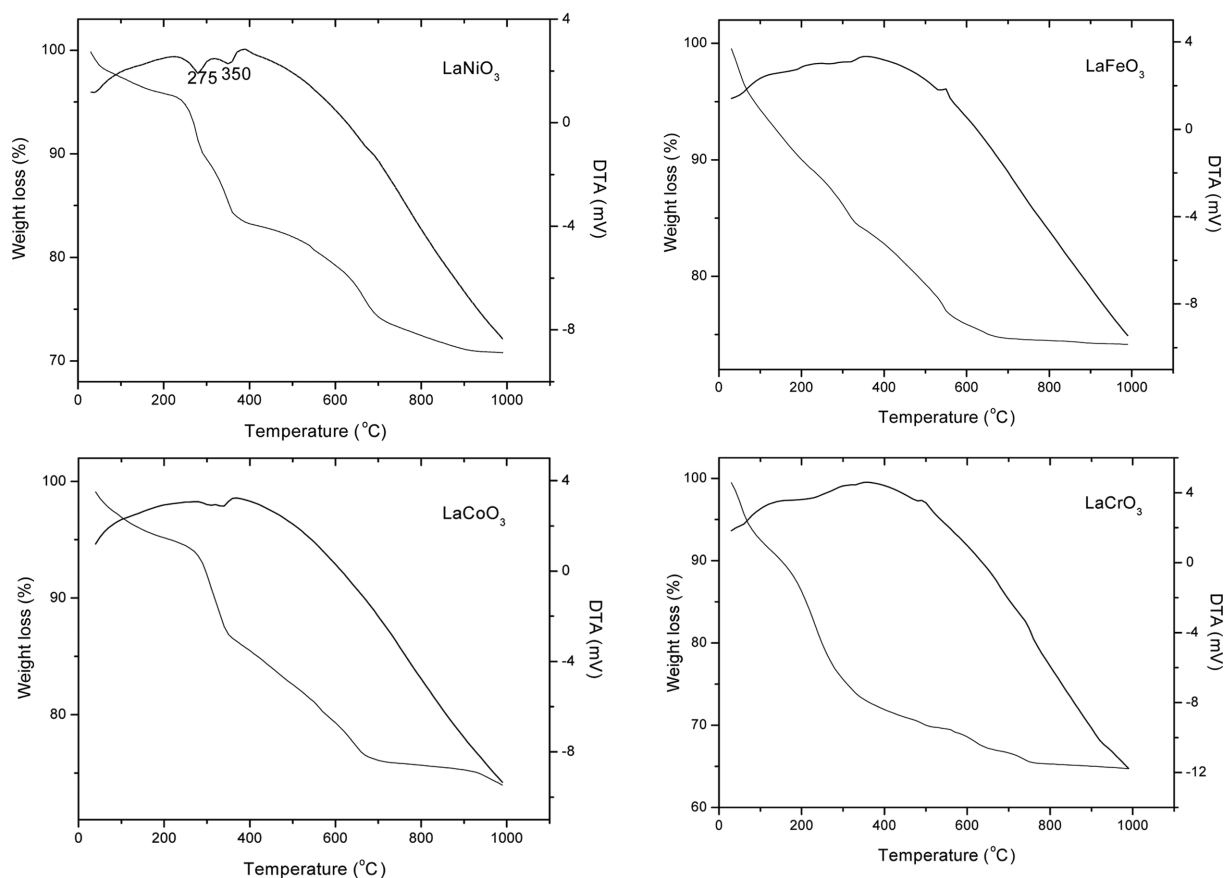


Fig. 4. TGA-DTA Curves corresponding to various solids prepared by coprecipitation.

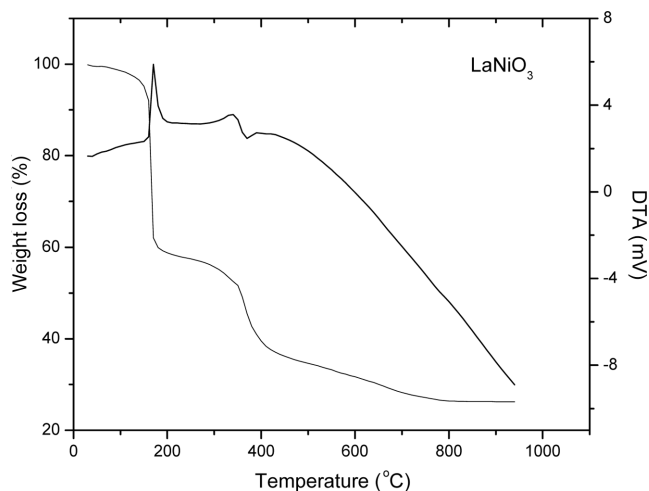


Fig. 5. TGA-DTA Curves corresponding to LaNiO_3 prepared by sol-gel.

(ii) the crystallite size of Perovskite phase prepared varied between 27-37 nm (c.f. Table 1); and (iii) LaCoO_3 and LaNiO_3 prepared by sol-gel have the lowest values of crystallite size 27 and 29 nm, respectively.

TEM micrographs in Fig. (3) show that the synthesis materials are a nanospherical morphology about 200 nm long while diameter ranges from 53-80 nm.

2. Thermal Analysis

The simultaneous DTA/TGA traces for uncalcined mixed solids in static air are shown in Figs. 4 and 5 consisting of two endothermic peaks. The maxima of these peaks are located at 200-275 °C and 325-350 °C. The first endothermic peak (located at about 200-275 °C) corresponds to the autocatalytic anionic oxidation reduction reaction between the nitrates and citric acid, yielding the mixed oxide solids.

The second endothermic peak found at about 350 °C indicates complete decomposition of the residual organic carbide. The two endothermic peaks were accompanied by weight losses of about 15% and 40%, respectively. So, the total weight loss taking place

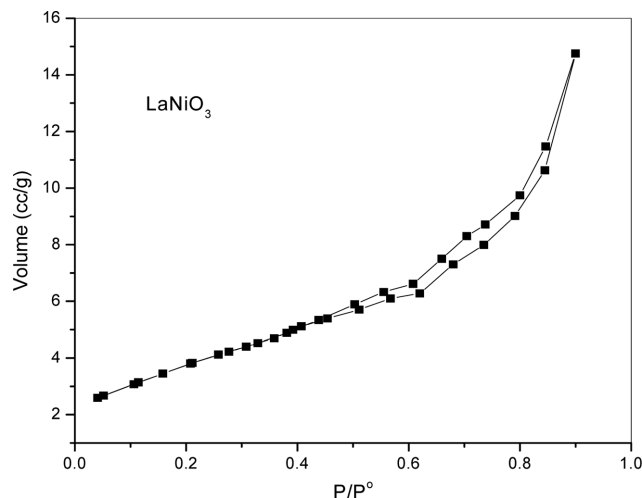


Fig. 7. Isotherm of LaNiO_3 prepared by sol-gel.

at temperature between 100 and 1,000 °C measured 55%.

3. Surface Characteristics of Different Solids

The surface characteristics, namely specific surface area (S_{BET}), total pore volume (V_p) and mean pore radius (r), of different adsorbents calcined at 700 °C were determined from analysis of nitrogen adsorption isotherms carried out at -196 °C. All isotherms belong to type II of Brunauer classification [19] having hysteresis loops of different shape and areas closing at P/P^0 at about 0.7. Figs. 6 and 7 depict representative adsorption-desorption isotherms of some investigated samples.

The computed values of S_{BET} , V_p and r are given in Table 2. Examination of Table 2 shows that (i) the S_{BET} of various solids varying between 21-34 m^2/g depending on the nature of the mixed oxides and its mode of preparation; (ii) the smallest S_{BET} were measured for LaFeO_3 and LaCoO_3 ; (iii) the mixed solids sample prepared by sol-gel (LaNiO_3) measured the biggest S_{BET} value; (iv) the mean pore radius (r) varies between 12.8-109 Å; and (v) LaNiO_3 prepared by sol-gel measured one of the smallest r value. So, the smallest pores and biggest surface area of LaNiO_3 prepared by sol-gel

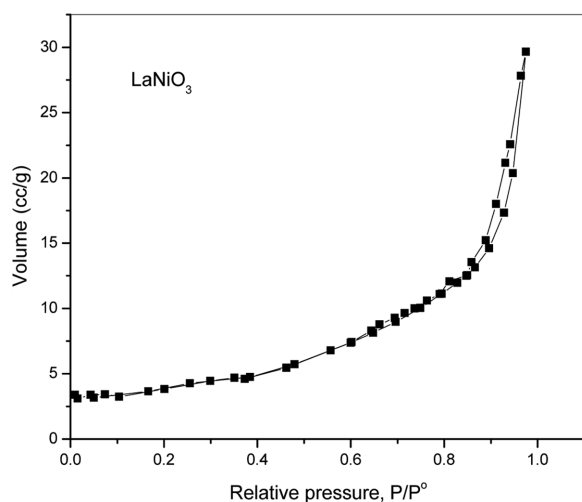


Fig. 6. Isotherms of some investigated samples prepared by coprecipitation.

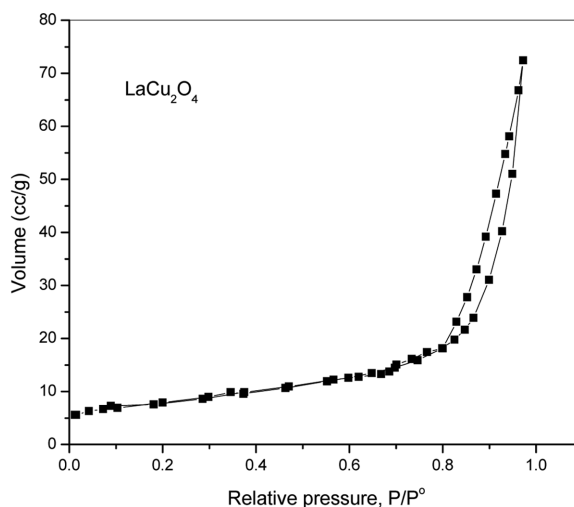


Table 2. Surface characteristics of variously mixed solids being calcined at 700 °C

Solids	S_{BET} m^2/g	Total pore volume $V_p, cc/g$	Mean pore radius r^- (nm)
LaNiO ₃ (coprecipitation)	29.0	0.048	33
LaNiO ₃ (sol-gel)	34.1	0.0232	13.6
LaFeO ₃	21.3	0.116	109
LaCoO ₃	21.4	0.02	21.5
LaCrO ₃	26.6	0.017	12.8
LaCu ₂ O ₄	27.6	0.116	84

might be expected to show the highest hydrogen adsorption capacity.

4. Hydrogen Storage

Hydrogen adsorption isotherms were measured at 100 °C for various prepared solids calcined at 700 °C. The obtained isotherms are illustrated in Fig. 8. It is seen from this figure that the amount of uptake hydrogen increases progressively by increasing the applied hydrogen pressure. The total amounts of adsorbed hydrogen over each sample were calculated from the maximum amount taken up at 20 bar of hydrogen pressure. The computed values are in Table 3. The amount of hydrogen stored in different solids increases according to the following sequence:

LaCoO₃ < LaFeO₃ < LaCrO₃ < LaCu₂O₄ < LaNiO₃ (prepared by copre-

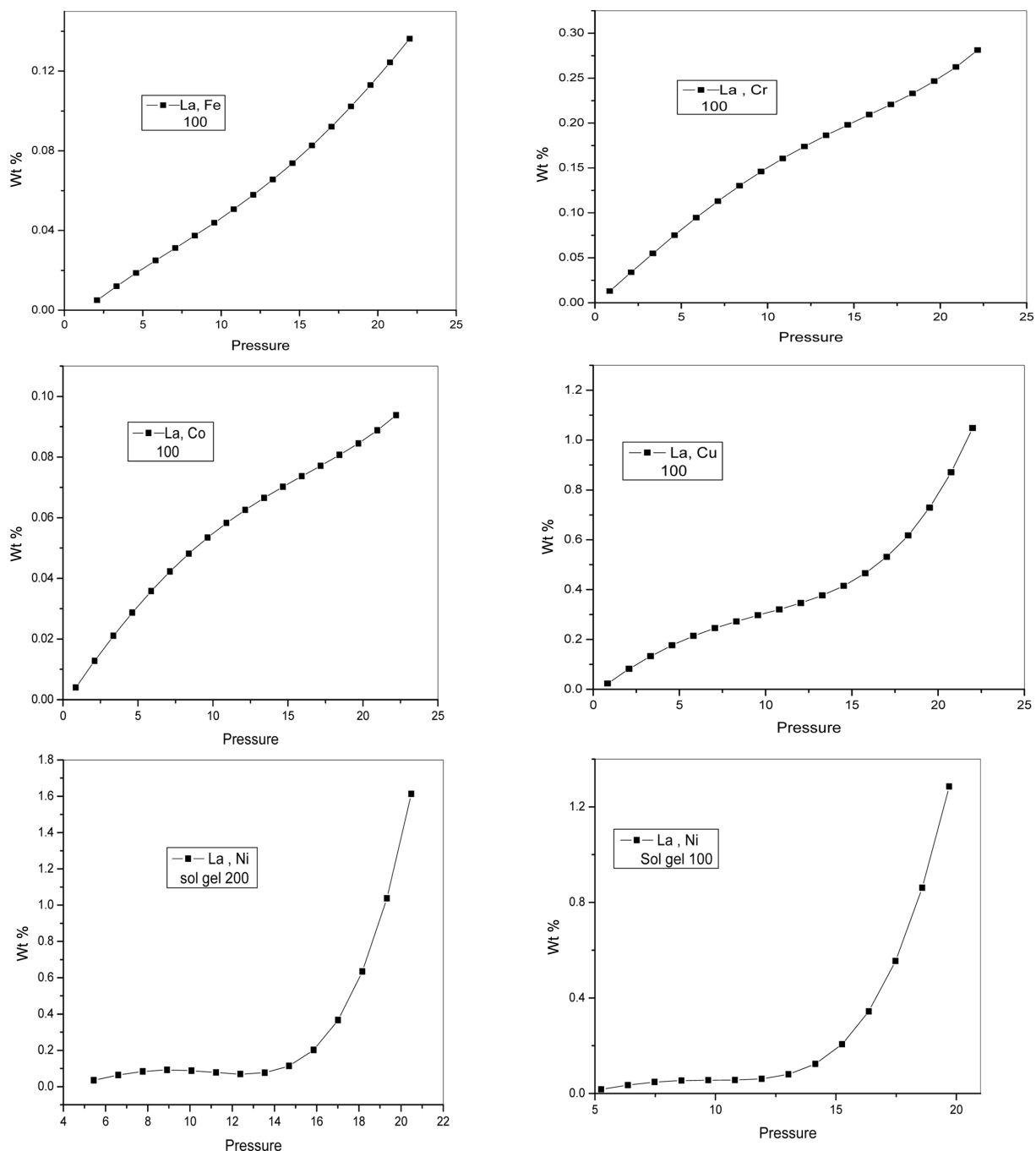


Fig. 8. Hydrogen absorption isotherms of various mixed solids.

Table 3. Hydrogen uptake of different mixed oxide solids measured at 100 °C and hydrogen pressure of 20 bar

Solids	Hydrogen uptake (wt%)
LaNiO ₃ (coprecipitation)	1.2
LaNiO ₃ (sol-gel)	1.7
LaFeO ₃	0.13
LaCoO ₃	0.09
LaCrO ₃	0.3
LaCu ₂ O ₄	1.1

cipitation) < LaNiO₃ (prepared by sol-gel)

So, the sample that has the highest specific surface area measure also has the highest hydrogen adsorption capacity at 100 °C and 20 bar, H₂ pressure.

It is clearly shown from the hydrogen adsorption measurement that the increase in the pressure of hydrogen above 20 bar might increase effectively the amount of hydrogen being uptaken. Furthermore, measuring the decrease of hydrogen measurement below 100 °C should lead to an increase in the adsorption capacity of hydrogen. On the basis of this speculation, LaNiO₃ prepared by sol-gel could be considered as a very promising material for hydrogen storage maybe because LaNiO₃ has the highest S_{BET} . The particles were examined using XRD before and after, not given, hydrogenation and the spectra showed no change in the structure, which ensured that no chemical change occurred for prepared particles under testing conditions. However, it is suggested that the layered platelet structure created interlayer spaces, which facilitates more hydrogen uptake.

CONCLUSIONS

The following are our main conclusions:

1. LaNiO₃, LaFeO₃, LaCoO₃, LaCu₂O₄ and LaCrO₃ were prepared by co-precipitation. An additional sample of LaNiO₃ was prepared by sol-gel. All samples were calcined at 700 °C.
2. All prepared solids exist as homogeneous nanosized phases with crystallite size between 27-37 nm.
3. All adsorbents are mesoporous solids with (r^*) values varying between 12.8-109 Å.
4. LaNiO₃ prepared by sol-gel method displays the highest specific surface area.
5. LaNiO₃ prepared by sol-gel and calcined at 700 °C exhibits the highest hydrogen adsorption capacity at 100 °C and hydrogen pressure of 20 bar.

ACKNOWLEDGEMENT

This work was supported by Al-Qassim University. The author expresses many thanks to the Deanship of scientific research for supporting this research.

REFERENCES

1. J. Germain, J. M. J. Frechet and F. Svec, *Small*, **5**, 1098 (2009).
2. D.-K. Lim, K.-C. Lee, C.-N. Park and S.-J. Song, *J. Ceramic Process. Res.*, **13**(3), 315 (2012).
3. Y. Gogotsi, C. Portet, S. Osswald, J. M. Simmons, T. Yildirim, G. Laudisio and J. E. Fischer, *Int. J. Hydrog. Energy*, **34**, 6314 (2009).
4. J. Dong, X. Wang, H. Xu, Q. Zhao and J. Li, *Int. J. Hydrog. Energy*, **32**, 4998 (2007).
5. K. S. Jung, E. Y. Lee and K. S. Lee, *J. Alloys Compds*, **421**(1-2), 179 (2006).
6. B. Sakintuna, F. Lamari-Darkrim and M. Hirscher, *Int. J. Hydrog. Energy*, **32**(9), 1121 (2007).
7. J. Li, S. Cheng, Q. Zhao, P. Long and J. Dong, *Int. J. Hydrog. Energy*, **34**, 1377 (2009).
8. M. H. Abdel Rehim, N. Ismail, A. A. Badawy and G. Turkey; *Mater. Sci. Eng. B*, **176**, 1184 (2011).
9. T. Esaka, H. Sakaguchi and Sh. Kobayashi, *Solid State Ionics*, **166**, 351 (2004).
10. S. M. Dorfman, Y. Meng, V. B. Prakapenka and T. S. Duffy, *Earth Planet. Sci. Lett.*, **361**, 249 (2013).
11. X. Tan, L. Shi, G. Hao, B. Meng and S. Liu, *Sep. Purif. Technol.*, **96**, 89 (2012).
12. E. Bontempia, C. Garzellab, S. Valettia and L. E. Deperoa, *J. Eur. Ceram. Soc.*, **23**, 2135 (2003).
13. R. C. Bowman Jr. and B. Fultz, *MRS Bulletin*, **37**, 688 (2003).
14. T. K. Mandal, L. Sebastian, J. Gopalakrishnan, L. Abrams and J. B. Goodenough, *MRS Bulletin*, **39**, 2257 (2003).
15. N. A. Merino, B. P. Barbero, P. Grange and L. E. Cadus, *J. Catal.*, **231**, 232 (2005).
16. S. Barison, M. Battagliarin, S. Daolio, M. Fabrizio, E. Miorin, P. L. Antonucci, S. Candamano, V. Modafferi, E. M. Bauer, C. Bellitto and G. Righini, *Solid State Ionics*, **177**, 3473 (2005).
17. H. Tanaka and M. Misono, *Current Opinion in Solid State and Materials Science*, **5**, 381 (2005).
18. B. D. Cullity, *Publishing Cos*, 2nd Ed., Addison-Wesley, Reading, MA (2005).
19. F. Rouquerol, J. Rouquerol and K. Sing, *Adsorption by powders and porous solids: Principles, methodology and applications*, Academic Press, San Diego (2005).